Structure formation in thermoresponsive microgel suspensions under shear flow

2004 J. Phys.: Condens. Matter 16 S3861

(http://iopscience.iop.org/0953-8984/16/38/006)

INSTITUTE OF PHYSICS PUBLISHING JOURNAL OF PHYSICS: CONDENSED MATTER

J. Phys.: Condens. Matter **16** (2004) S3861–S3872 PII: S0953-8984(04)77444-5

Structure formation in thermoresponsive microgel suspensions under shear flow

Markus Stieger[1], **Peter Lindner**[2] **and Walter Richtering**[3,4]

[1] Institute of Physical Chemistry, University of Kiel, Olshausenstraße 40, D-24098 Kiel, Germany
[2] Institute Laue-Langevin, 6 rue Jules Horowitz, BP 156-38042, Grenoble, Cedex 9, France
[3] Institute of Physical Chemistry II, RWTH Aachen University, Templergraben 59, D-52056 Aachen, Germany

E-mail: richtering@rwth-aachen.de

Received 5 March 2004
Published 10 September 2004
Online at stacks.iop.org/JPhysCM/16/S3861
doi:10.1088/0953-8984/16/38/006

Abstract

Shear-induced structures of concentrated temperature-sensitive poly(*N*-isopropylacrylamide) (PNiPAM) microgel suspensions have been studied employing small angle neutron scattering (rheo-SANS). The interaction potential of swollen PNiPAM microgels could be varied from repulsive at temperatures below the lower critical solution temperature to attractive at temperatures above the lower critical solution temperature. In contrast to the case for suspensions of rigid spheres, the effective volume fraction could be changed by means of temperature while the mass concentration and particle number density were kept constant. Thus, aqueous PNiPAM microgels are interesting model systems with unique colloidal properties. Complementary information about shear-induced changes of both the internal particle structure and the overall microstructural phenomena were obtained from rheo-SANS experiments with PNiPAM microgels with different particle sizes. The shear-induced particle arrangements strongly depended on the particle–particle interaction potential. When the interaction potential was repulsive at temperatures below the lower critical solution temperature, no significant deformation of the swollen PNiPAM particles was observed even at high shear rates. Shear-induced ordering was found at high shear rates resulting in the formation of two-dimensional hexagonal close packed layers that aligned along the flow direction giving rise to shear thinning. The formation of sliding hexagonal close packed layers under shear flow is therefore proposed to be a general property of colloidal dispersion independent of the internal structure of the particle. At temperatures near the lower critical solution temperature, when the particle interaction potential is not yet strongly attractive, shear flow induces the collapse of an individual particle in concentrated suspension at high

[4] Author to whom any correspondence should be addressed.

0953-8984/04/383861+12$30.00

shear rates. A so-called butterfly scattering pattern indicates the shear-induced enhancement of concentration fluctuations along the flow direction leading to solvent being squeezed out of the particles until phase separation occurs finally.

(Some figures in this article are in colour only in the electronic version)

1. Introduction

Colloidal microgels have attracted great interest as model systems in soft condensed matter science for studying the structure and dynamics of concentrated suspensions [1]. In particular, the equilibrium phase behaviour and rheology have been thoroughly investigated [2, 3]. Usually, microgels are prepared by emulsion polymerization techniques. Microgels can be considered intermediates between sterically stabilized colloids and macroscopic polymer gels. Like colloids, spherical microgels are usually limited to mesoscopic dimensions ranging from several nanometres to a few microns. But in contrast to conventional latex dispersions, microgels are chemically cross-linked particles that are swollen by a good solvent and due to their lyophilic character no special stabilization is needed to avoid aggregation. The internal structure of a microgel is that of a swollen polymer network and can be compared with macroscopic gels.

Thermoresponsive microgels facilitate control of a large variety of colloidal properties by means of temperature. Water-swellable microgels consisting of poly(*N*-isopropylacrylamide) (PNiPAM) are known to undergo a temperature-induced volume phase transition when the lower critical solution temperature (LCST) of about 33 °C is approached [4, 5]. At temperatures below the LCST water is a good solvent and the particles are highly swollen. At elevated temperatures the solvent quality changes and above the LCST water is a non-solvent leading to the collapse of the particles and eventually phase separation in concentrated suspension. Thus, a major advantage of thermoresponsive PNiPAM microgels is that the particle–particle interaction potential can be controlled by temperature [6, 7]. The interaction potential is repulsive at temperatures well below the LCST and does not change significantly up to approximately 1 K below the LCST. At temperatures above the LCST, the interaction potential becomes attractive. The size of the particle decreases with increasing temperature. Hence, an additional interesting property of PNiPAM microgels is that the effective volume fraction ϕ_{eff} can easily be controlled by means of simple temperature changes while the mass concentration c and thus the particle number density n are kept constant [8]. The degree of swelling changes with temperature and the rigidity of the particles is expected to depend on temperature as well.

Since colloidal dispersions play an important role in many different industrial applications, the rheological behaviour and flow properties have been studied intensively [9]. Colloidal dispersions under shear reveal a large variety of distinct changes of the particle arrangement with shear rate. The shear-induced structures depend strongly on the particle–particle interaction potential. Various methods including light and small angle neutron investigations were employed to study the flow-induced structures in colloidal systems with different interaction potentials. The formations of different structures during flow have been predicted by non-equilibrium molecular dynamics simulations without hydrodynamic interaction [10] and by Stokesian dynamics simulations including hydrodynamic interactions [11]. For both purely repulsive hard spheres [12–14] and electrostatic stabilized particles [15–17], shear thinning is often observed in concentrated dispersions. After application of shear flow a structural transition from fluid-like particle ordering to two-dimensional hexagonal close packed (2D hcp)

layers occurs; these latter are arranged to minimize the resistance against flow [12–17]. The shear thickening in hard sphere and electrostatic stabilized suspensions which occurs when high shear rates are applied can be attributed to the formation of jamming clusters bound together by hydrodynamic lubrication forces, often referred to as hydroclusters [18]. For a wide range of colloidal suspensions with an attractive interaction potential or weakly aggregating suspensions, butterfly scattering patterns have been reported during shear flow and it was suggested that a shear-induced demixing process is responsible for the development of those patterns [19–21]. Similar arguments were employed by Hobbie *et al* [22] suggesting that coupling between composition and shear stress leads to demixing. However, Hoekstra *et al* [23] have demonstrated for two-dimensional attractive suspensions that a purely hydrodynamic mechanism due to break-up and re-aggregation of flocks leads to the development of structural anisotropy. The influence of shear flow on the structure of gel-forming sticky hard spheres was studied by Verduin *et al* [24]. At low shear rates the formation of larger structures aligned mainly along the flow direction was observed. At higher shear rates the cloud point was shifted. Occasionally, shear flow in colloidal systems can also lead to aggregation or the formation of large scale bundle ordering [25]. Shear-induced distortions of the microstructure in directions perpendicular to the flow were observed in near-critical suspensions of colloid–polymer mixtures under stationary shear flow [26]. Especially in the vicinity of the gas–liquid critical point, the influence of shear flow on the concentration fluctuations was found to be substantial [27].

To our knowledge very little is known about the influence of shear flow on the structure of suspensions of thermoresponsive microgels. Unlike the case for suspensions of rigid spheres, the effective volume fraction ϕ_{eff} of microgel suspensions changes with temperature [8]. The liquid–solid transition is shifted to higher concentrations with increasing temperature, due to particle collapse at temperatures above the LCST. Particle collapse occurs due to the changing of the interaction potential from repulsive to attractive, which is in turn a result of decreasing solvent quality. Previously, we observed shear-induced phase separation for aqueous suspensions of PNiPAM microgels [28]. Changes in the cloud curve under shear flow were present when the particle density was sufficiently high to be above the liquid–solid transition. The solvent squeezing mechanism, which describes the dynamic coupling between concentration fluctuations and stress, seems to describe this phenomenon [29].

In this contribution we address the question of whether the differing colloidal properties of PNiPAM microgels as compared to rigid spheres give rise to different particle arrangements under shear flow. Two PNiPAM microgels with different particle sizes but similar cross-linking density (M-1.4/141 and M-1.5/353) were investigated by means of small angle neutron scattering under various shear conditions (rheo-SANS). The scattering intensity distributions $I(q)$ were obtained in the q-region of about $0.0008\ \text{Å}^{-1} < q < 0.006\ \text{Å}^{-1}$ where q denotes the magnitude of the momentum transfer. For the large particles (M-1.5/353), the main contribution to the overall scattering intensity $I(q)$ in this q-region arises from contributions of the particle form factor $P(q)$. Hence, detailed information about the influence of shear flow on the internal structure of an individual particle in concentrated suspension is obtained from scattering experiments with the M-1.5/353 sample. Under shear the highly swollen particles might be deformed. In the case of the small PNiPAM particles (M-1.4/141), the scattering intensity distribution $I(q)$ in this q-region is dominated by contributions of the structure factor $S(q)$. Thus, studying the small M-1.4/141 particles leads to information about changes in the overall microstructure and shear-induced ordering. Both microgels were studied at temperatures well below and close to the LCST to reveal the influence of the particle–particle interaction potential on the shear-induced structure formation. In addition, the rheological behaviour will be presented.

2. Experimental details

Synthesis and characterization of the PNiPAM microgels has been described elsewhere [8, 28, 30, 31]. In this work, a standard naming procedure for the PNiPAM microgels is followed: the two numbers in the sample name refer to the degree of cross-linking, as the molar ratio of cross-linker to monomer, and to the hydrodynamic radius in nm at 25 °C in heavy water obtained by means of dynamic light scattering. For example, the M-1.4/141 microgel exhibits a cross-linking density of 1.4 mol % cross-linker *N*,*N*′-methylenbisacrylamide and a hydrodynamic radius of $R_h(25\,°C) = 141$ nm.

Small angle neutron scattering experiments under shear (rheo-SANS) were performed at the instrument D11 of the Institut Laue-Langevin (ILL) in Grenoble, France. The neutron wavelength was $\lambda = 6$ or 12 Å with a spread of $\Delta\lambda/\lambda = 9\%$. The data were collected on a two-dimensional multidetector (64×64 elements of 1×1 cm^2) at a sample–detector distance of 36.7 m. The data were corrected for background and empty cell scattering. A Bohlin CVO-120-HR rheometer was adjusted to the D11 beamline. Measurements were performed using a Searle shear cell of quartz cylinders with a gap of 1 mm. The scattering experiments were performed in the radial position yielding information in the plane formed by the flow and vorticity directions. To obtain a one-dimensional data set $I(q)$, further processing of the two-dimensional SANS pattern was done by radially averaging in the flow and vorticity directions employing a radial sector analysis with an opening angle of $\Delta\varphi = 10°$ and using software available at the ILL ($GRAS_{ans}P$ V. 3.25). Azimuthal intensity distributions $I(\varphi)$ were obtained by averaging in a 270° or 360° sector with an angular bin of 4° or 6° covering different q-regions as indicated. All experiments were carried out at full contrast using D_2O as the solvent.

3. Results and discussion

3.1. Shear-induced structures at temperatures well below the LCST

The first aspect of this work is a description of the behaviour of swollen PNiPAM microgels under shear at temperatures well below the LCST. Results from 25.0 and 28.5 °C will be presented. At those temperatures, the interaction potential is purely repulsive. We first present data on the internal structure of the particles, then the flow-induced microstructural changes. Since the M-1.5/353 microgel particles are rather large, the main contribution to the overall scattering intensity distribution with this sample in the q-region investigated arises from contributions of the form factor $P(q)$. The scattering intensity distributions $I(q)$ obtained from the large microgel at a concentration of 8.0 wt% at rest (filled symbols) and under sheared conditions (open symbols) are presented in figure 1. The two-dimensional scattering patterns were averaged radially along the flow (squares) and neutral (stars) direction. No significant changes were observed in $I(q)$ obtained from averaging procedures along both directions when shear flow was applied. The sample was shear thinning, but the scattering patterns remained isotropic even at high shear rates. In the quiescent state and under shear the scattered intensity $I(q)$ exhibits pronounced form factor minima at similar q-values. This indicates that no significant deformation of an individual, highly swollen microgel particle occurs in concentrated suspension after application of shear flow.

Since the 2D SANS patterns of the large M-1.5/353 were isotropic, experimental intensity distributions $I(q)$ with small statistical errors could be obtained from radial averaging procedures over the entire spectra. The previously established model expression for the particle form factor $P(q)$ and structure factor $S(q)$ for concentrated PNiPAM microgel suspensions described the experimental data at rest and under shear $I(q)$ well [7, 30]. Since the q-range

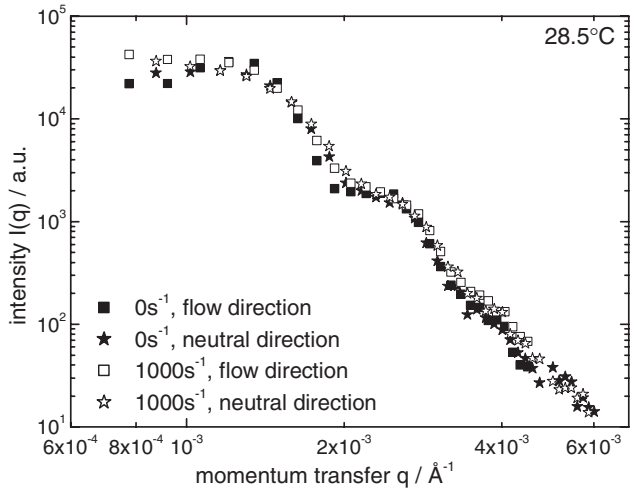

Figure 1. The scattering intensity distribution $I(q)$ for the M-1.5/353 at $T = 28.5\,^{\circ}\mathrm{C}$ and a concentration of 8.0 wt%. The filled symbols represent data obtained at rest and the open symbols the data obtained under shear flow. The squares show the data along the flow direction; the stars represent the neutral direction.

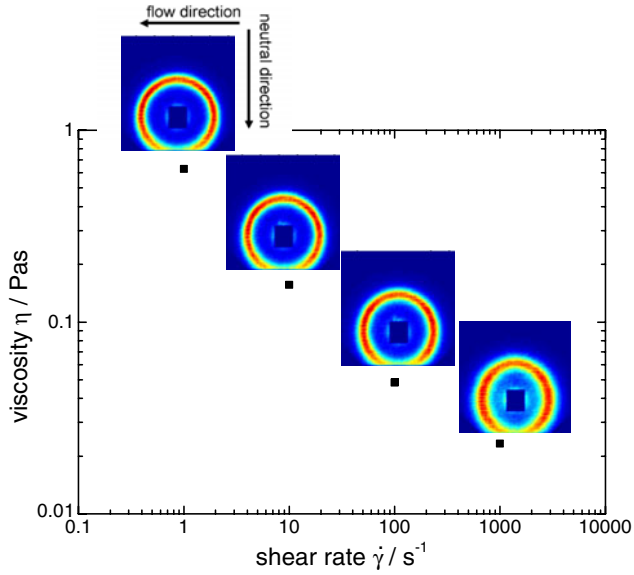

Figure 2. 2D SANS patterns and viscosity versus shear rate for the M-1.4/141 at 25 °C and a concentration of 3.6 wt%.

investigated under shear was limited compared to those in our previous studies in the quiescent state, the fitting parameters obtained under shear must be interpreted cautiously. However, the particle radius R, the width of the smeared particle surface σ_{suf}, the particle size polydispersity σ_{poly} and the polymer volume fraction in the centre of a particle $\phi(r = 0)$ determined under shear were generally in fairly good agreement with the data obtained at rest. The SANS data obtained at a concentration of 8.0 wt% of the M-1.5/353 microgel are similar to the previously described scattering profiles $I(q)$ of a 10.0 wt% sample of the same microgel [28].

In contrast to the case for the larger M-1.5/353 microgel, the main contribution to the overall scattering intensity of the small M-1.4/141 sample in the low q-region arises from the structure factor $S(q)$. Thus, information about shear-induced changes in the overall microstructure can be gained from scattering experiments with the small PNiPAM microgels. 2D SANS patterns for the small microgel in combination with the flow curve at 25.0 °C under various sheared conditions at a concentration of 3.6 wt% are shown in figure 2. This microgel

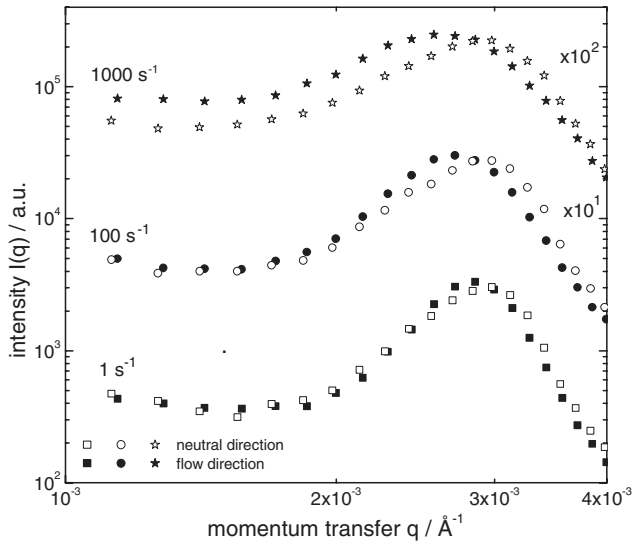

Figure 3. The scattering intensity distribution $I(q)$ for the M-1.4/141 at 25 °C and a concentration of 3.6 wt% at various shear rates. The open symbols represent data obtained along the neutral direction; the filled symbols represent the flow direction. For the sake of clarity some of the data sets were multiplied by constant factors.

sample formed colloidal crystals in the quiescent state at this temperature and concentration. Shear thinning was observed and the viscosity η decreased by a factor of 40 when the shear rate was increased from $\dot{\gamma} = 1$ to 1000 s^{-1}. The 2D SANS patterns reveal the maximum of the structure factor $S(q)$ as a ring. To characterize the anisotropy of the scattering pattern under shear flow the structure factor $S(q)$ was expanded into spherical harmonics according to the procedure described by Wagner *et al* [32, 33]. At a low shear rate ($\dot{\gamma} = 1$ s^{-1}) the scattering pattern reveals no significant anisotropy in the harmonic expansion. At higher shear rates ($\dot{\gamma} = 100$ and 1000 s^{-1}) a strong anisotropy of the pattern evolves, which is quantified by the averaged intensity distributions $I(q)$ along the neutral and flow directions that are shown in figure 3. A broadening of the structure factor peak is observed in both the neutral and flow directions with increasing shear rate. When shear flow is applied, the maximum of the structure factor determined along the flow direction is shifted towards smaller q-values, whereas the peak position obtained along the neutral direction remains unchanged at a position of approximately $q = 0.0029$ $Å^{-1}$. This indicates that the average particle–particle distance along the flow direction increases at high shear rates without changing the distance along the neutral direction.

The 2D SANS patterns accompanied by the flow curve for a more concentrated suspension of the small M-1.4/141 microgel are shown in figure 4. The microgel suspension was in the glassy state at 25.0 °C at a concentration of 7.0 wt%. At high concentrations shear thinning is more pronounced and a decrease of the viscosity η by a factor of about 100 was found when the shear rate was increased from $\dot{\gamma} = 1$ to 1000 s^{-1}. As for the less concentrated sample, broadening of the structure factor maximum and shift of the peak position along the flow direction towards smaller q-values is observed. In addition, a highly ordered superstructure is observed at a shear rate of $\dot{\gamma} = 100$ s^{-1} indicated by four sharp Bragg peaks at the ($1\underline{1}$), (01), ($0\underline{1}$) and ($\underline{1}1$) positions [16, 34]. This clearly indicates a sliding layer motion of two-dimensional hexagonal close packed (2D hcp) layers, which gives rise to a significant decrease of viscosity η with increasing shear rate. The experimentally observed 2D SANS patterns are in good agreement with calculated scattering patterns [34]. Similar shear-induced structures have been observed by different groups in suspensions of hard spheres [13] and electrostatic stabilized lattices [15, 16] at various shear rates in the shear thinning region. We therefore

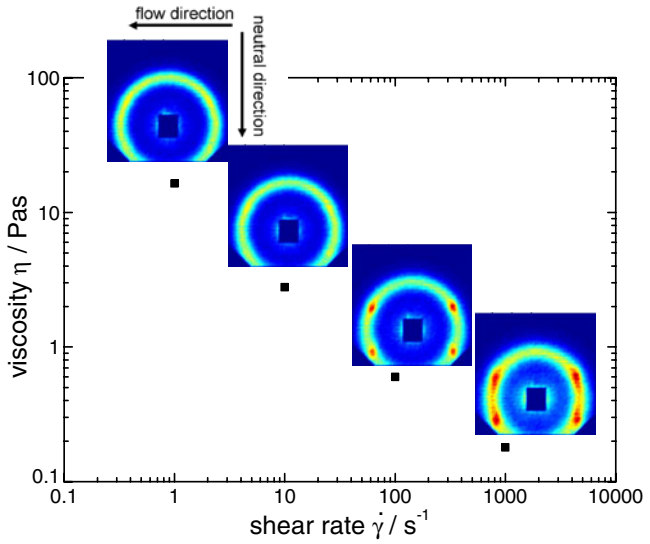

Figure 4. 2D SANS patterns and viscosity versus shear rate for the M-1.4/141 at 25 °C and a concentration of 7.0 wt%.

conclude that the formation of sliding hexagonal close packed layers under shear flow is a general property of colloidal dispersions independent of the internal structure of the particle. The corresponding azimuthal averaged intensity distributions $I(\varphi)$ are depicted for different shear rates in figure 5. At $\dot{\gamma} = 1000\ \mathrm{s}^{-1}$ the sliding motion of the hcp layers is slightly distorted in favour of a more liquid-like structure which can be seen by a broadening of the Bragg peaks. The positions of the Bragg peaks do not change significantly with increasing shear rate and are observed at angles of approximately $\varphi = 60°$ and 120°. It should be noted that in the 2D SANS patterns at low shear rates ($\dot{\gamma} = 1$ and $10\ \mathrm{s}^{-1}$) in figure 4 significant Bragg peaks were absent. The glassy microgel suspension was shear thinning in the low shear rate region although the formation of sliding layers was not indicated by the scattering data. Using a mode coupling approach, Fuchs *et al* [35] have demonstrated that in colloidal glasses the structural relaxation is speeded up under small shear flow and the caging of particles is suppressed. The predicted cage-breaking particle motion might explain the experimentally observed shear thinning at small shear rates.

The anisotropic scattering intensity distributions $I(q)$ of the small M-1.4/141 microgel presented in this contribution could not be reasonably described with the previously established model for the structure factor $S(q)$, since the model expression does not account for anisotropy of the scattering intensity $I(q)$ [7, 30]. The volume fractions of the M-1.4/141 suspensions studied under flow were outside the expected validity range of the Percus–Yevick approximation for the structure factor, which was used in the model.

3.2. Structure formation under flow at temperatures near the LCST

The second aspect of this work is to investigate the influence of shear flow on the behaviour of PNiPAM microgels at temperatures near the LCST. Data obtained at 32.0 and 32.5 °C will be presented. At those temperatures, the interaction potential at rest is not yet strongly attractive, but can no longer be said to be purely repulsive. First data on the internal structure and then changes of the microstructure are discussed. Figure 6 shows the scattering intensity $I(q)$ obtained from a 8.0 wt% suspension of the large M-1.5/353 microgel at rest (filled symbols) and under shear (open symbols). Again, the scattering patterns revealed no anisotropy even

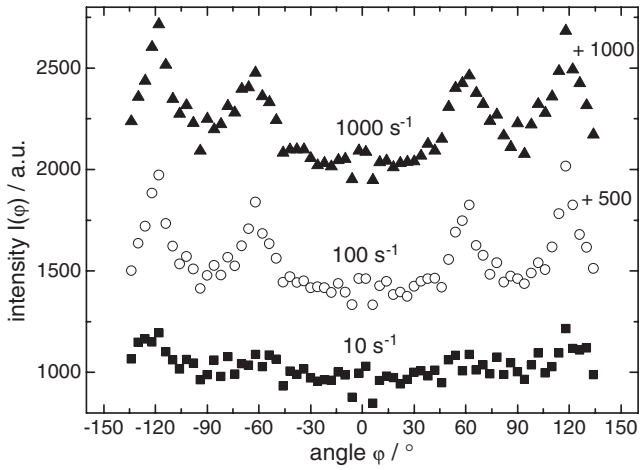

Figure 5. The azimuthal intensity distribution $I(\varphi)$ for the M-1.4/141 at 25 °C and a concentration of 7.0 wt% at various shear rates. $I(\varphi)$ was obtained by averaging in a 270° sector with an angular bin of 4° covering the q-range from 0.0026 Å^{-1} $< q <$ 0.0041 Å^{-1}. For the sake of clarity constants were added to some of the data sets as indicated.

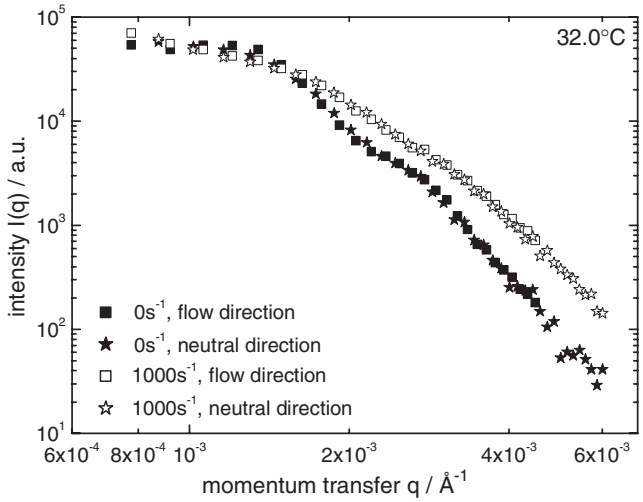

Figure 6. The scattering intensity distribution $I(q)$ for the M-1.5/353 at $T = 32.0$ °C and a concentration of 8.0 wt%. The filled symbols represent data obtained at rest and the open symbols the data obtained under shear flow. The squares show the data along the flow direction; the stars represent the neutral direction.

at high shear rates and the data obtained in flow and neutral directions fell on a single curve. The individual microgel particles reveal no significant deformation under shear, but a strong increase of $I(q)$ in the high q-region of 0.002 Å^{-1} $< q <$ 0.006 Å^{-1} is observed when the suspension is sheared. The minima of the form factor $P(q)$ observed at rest vanish when shear flow is applied. Experimental intensity distributions $I(q)$ with small statistical errors were obtained from radial averaging procedures over the entire spectra, then described at rest and under shear by the previously established model expression [7, 30]. As mentioned before, due to the limited q-range investigated under shear, care must be taken in discussing the absolute

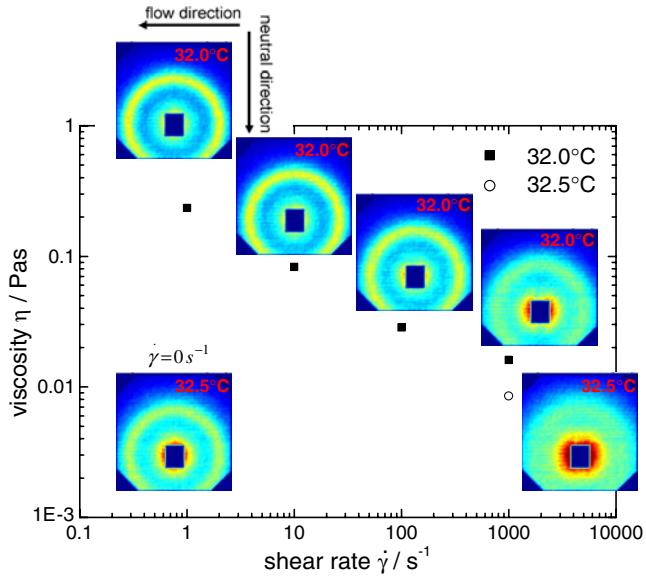

Figure 7. 2D SANS patterns and viscosity versus shear rate for the M-1.4/141 at 32.0 and 32.5 °C at a concentration of 7.0 wt%.

values obtained from the fitting procedures under shear. However, compared to the quiescent state, shear flow provoked a decrease of the particle radius from $R_{32\,^\circ\mathrm{C}}(\dot\gamma = 0\,\mathrm{s}^{-1}) = 298$ nm to $R_{32\,^\circ\mathrm{C}}(\dot\gamma = 1000\,\mathrm{s}^{-1}) = 167$ nm and an increase of the polymer volume fraction in the centre of a particle from $\phi_{32\,^\circ\mathrm{C}}(r = 0, \dot\gamma = 0\,\mathrm{s}^{-1}) = 0.04$ to $\phi_{32\,^\circ\mathrm{C}}(r = 0, \dot\gamma = 1000\,\mathrm{s}^{-1}) = 0.09$ accompanied by a dramatic sharpening of the width of the smeared particle surface from $\sigma_{\mathrm{suf},32\,^\circ\mathrm{C}}(\dot\gamma = 0\,\mathrm{s}^{-1}) = 23$ nm to $\sigma_{\mathrm{suf},32\,^\circ\mathrm{C}}(\dot\gamma = 1000\,\mathrm{s}^{-1}) = 3$ nm. This reveals the shear-induced collapse of individual particles in concentrated suspension. We emphasize that results determined at a shear rate of $\dot\gamma = 1000\,\mathrm{s}^{-1}$ approximately 1 K below the LCST agree qualitatively with the data obtained previously in the quiescent state at temperatures above the LCST. This demonstrates nicely that the influence of shear flow on the phase separation process near the miscibility gap is similar to a temperature increase. This is in good agreement with the SANS data obtained recently at a concentration of 10.0 wt% for the M-1.5/353 [28].

The rheo-SANS experiments provide information about the internal structure of a single particle in concentrated suspension. Apparently, shear flow induces the particle collapse at temperatures near the LCST. However, previously described rheo-turbidity experiments revealed no shift of the cloud point temperature under shear flow for this concentration [28]. A shear-induced shift of the cloud point temperature was found only for concentrations of 10.0 wt% or higher. The rheo-turbidity measurements reveal the macroscopic shear-induced phase separation. Shear-induced demixing was only observed when the concentration of the microgel suspension was so high that the sample had dominant elastic properties at temperatures near the LCST. This may indicate that the demixing process starts at a local, microscopic level on small length scales which is detected by rheo-SANS before it is observed macroscopically in rheo-turbidity experiments [36].

The flow curve in combination with the 2D SANS patterns at 32.0 and 32.5 °C for the 7.0 wt% suspension of the small M-1.4/141 microgel is shown in figure 7 and shear thinning is observed again. At high shear rates of $\dot\gamma = 100$ and $1000\,\mathrm{s}^{-1}$ a pronounced anisotropy evolves in the low q-region. The increase in scattering intensity $I(q)$ along the flow direction relative to the neutral direction under shear is shown in figure 8 for both temperatures. In addition, the peak of the structure factor that is visible at rest and small shear rates vanished

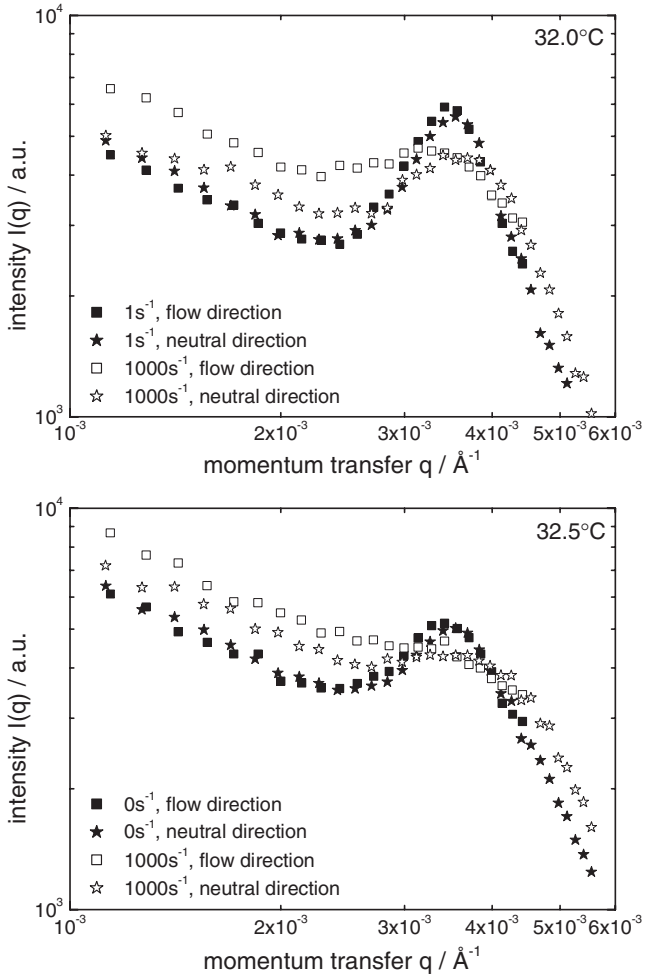

Figure 8. The scattering intensity distribution $I(q)$ for the M-1.4/141 at 32.0 °C (top) and 32.5 °C (bottom) and a concentration of 7.0 wt% at different shear rates. The filled symbols represent data obtained at rest or very small shear rates and the open symbols the data obtained at high shear rates. The squares show the data along the flow direction; the stars represent the neutral direction.

almost entirely upon application of shear flow. This can be compared with SANS experiments performed with concentrated thermoresponsive PNiPAM microgels at rest. In the quiescent state, particle collapse is induced when the temperature is raised above the LCST [30]. The peak of the structure factor which was observed at temperatures below the LCST vanished at elevated temperatures. This demonstrates again that shear-flow-induced phase separation. However, the scattering patterns obtained at rest were always isotropic. The anisotropy in the scattering intensity in the low q-region provoked by high shear rates is depicted in more detail in the azimuthal averaged intensity distributions $I(\varphi)$ which are shown in figure 9. At rest and small shear rates of $\dot{\gamma} = 10\ \mathrm{s}^{-1}$ the expansion of the structure factor into spherical harmonics reveals no significant anisotropy. At high shear rates of $\dot{\gamma} = 1000\ \mathrm{s}^{-1}$ a twofold-symmetric intensity distribution $I(\varphi)$ indicated the presence of a so-called butterfly pattern in the low q-region consisting of two lobes along the flow direction. The application of

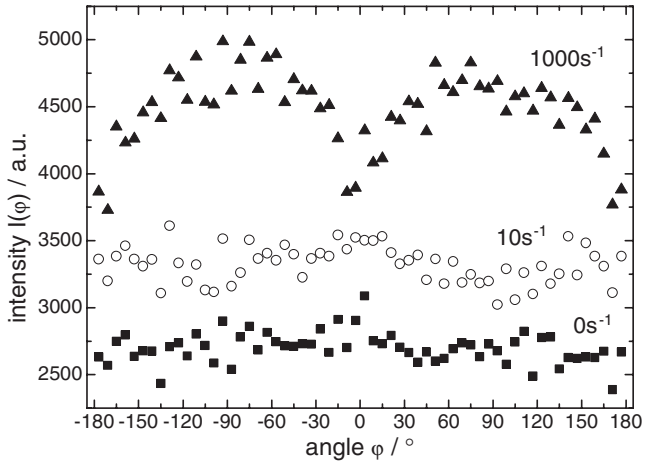

Figure 9. The azimuthal intensity distribution $I(\varphi)$ for the M-1.4/141 at 32 °C and a concentration of 7.0 wt% at various shear rates. $I(\varphi)$ was obtained by averaging in a 360° sector covering the q-range from 0.0015 Å^{-1} $< q <$ 0.002 Å^{-1} with an angular bin of 6°.

shear flow apparently led to an enhancement of concentration fluctuations along the flow direction indicated by the butterfly pattern. A solvent squeezing mechanism may therefore be responsible for the shear-induced demixing at high concentrations. When the particles are densely packed, stress relaxation via particle diffusion is hindered. The coupling between concentration fluctuations and shear stress can result in squeezing solvent out of the particle giving rise to an enhancement of concentrations fluctuations and turbidity eventually leading to shear-induced phase separation.

4. Conclusions

Thermoresponsive PNiPAM microgels are interesting model systems for concentrated suspensions with unique colloidal properties. The interaction potential of thermoresponsive PNiPAM microgels can be varied from repulsive at temperatures below the LCST to attractive at temperatures above the LCST. In contrast to the case for suspensions of rigid spheres, the effective volume fraction can be changed by means of temperature while the mass concentration and particle number density are kept constant. Above the LCST the microgel particles eventually collapse.

Investigating PNiPAM microgels with different particle sizes in the same q-region provides complementary information about shear-induced changes of both the internal particle structure and the overall microstructural phenomena. The shear-induced particle arrangements strongly depend on the interaction potential. When the interaction potential is repulsive at temperatures below the LCST, individual swollen PNiPAM particles in concentrated suspension are not deformed significantly even at high shear rates. Shear-induced ordering is observed at high shear rates resulting in the formation of two-dimensional hexagonal close packed layers that align along the flow direction giving rise to shear thinning. The formation of sliding hexagonal close packed layers under shear flow is therefore proposed to be a general property of colloidal dispersion independent of the internal structure of the particle. At temperatures near the LCST, when the particle interaction potential is not yet strongly attractive, shear flow induces the collapse of an individual particle in concentrated suspension at high shear rates. The

particle collapse is accompanied by a sharpening of the width of the segment density profile at the particle surface. A so-called butterfly scattering pattern indicates the shear-induced enhancement of concentration fluctuations along the flow direction and phase separation occurs finally. Shear-induced demixing has also been observed in aqueous solutions of linear chain PNiPAM by means of rheo-SANS and rheo-turbidity [28, 37].

Acknowledgments

We are greatly indebted to Jan Skov Pedersen, University of Aarhus, Denmark, for his contributions to the development of the model for the scattering intensity and rewarding discussions. Financial support by the Deutsche Forschungsgemeinschaft is gratefully acknowledged.

References

[1] Antonietti M 1988 *Angew. Chem.* **27** 1743
[2] Bartsch E, Kirsch S, Lindner P, Scherer T and Stölken S 1998 *Ber. Bunsenges. Phys. Chem.* **11** 1597
[3] Eckert T and Bartsch E 2002 *Phys. Rev. Lett.* **89** 125701
[4] Schild H G 1992 *Prog. Polym. Sci.* **17** 163
[5] Saunders B R and Vincent B 1999 *Adv. Colloid Interface Sci.* **80** 1
[6] Wu J, Huang G and Hu Z 2003 *Macromolecules* **36** 440
[7] Stieger M, Pedersen J S, Lindner P and Richtering W 2004 *Langmuir* **20** 7283
[8] Senff H and Richtering W 1999 *J. Chem. Phys.* **111** 1705
[9] Mellema J 1997 *Curr. Opin. Colloid Interface Sci.* **2** 411
[10] Loose W and Hess S 1989 *Rheol. Acta* **28** 91
[11] Bossis G and Brady J F 1984 *J. Chem. Phys.* **80** 5141
[12] Ackerson B J, Hayter J B, Clark N A and Cotter L 1986 *J. Chem. Phys.* **84** 2344
[13] Ackerson B J and Pusey P N 1988 *Phys. Rev. Lett.* **61** 1033
[14] Chen L B, Zukoski C F, Ackerson B J, Hanley H J M, Straty G C, Barker J and Glinka G J 1992 *Phys. Rev. Lett.* **69** 668
[15] Laun H M, Bung R, Hess S, Loose W, Hess O, Hahn K, Hädicke E, Hingmann R, Schmidt F and Lindner P 1992 *J. Rheol.* **36** 743
[16] Dux Ch, Musa S, Reus V, Versmold H, Schwahn D and Lindner P 1998 *J. Chem. Phys.* **109** 2556
[17] Versmold H, Musa S and Bierbaum A 2002 *J. Chem. Phys.* **116** 2658
[18] Young S L and Wagner N J 2003 *Rheol. Acta* **42** 199
[19] Varadan P and Solomon M J 2001 *Langmuir* **17** 2918
[20] DeGroot J V, Macosko C W, Kume T and Hashimoto T 1994 *J. Colloid Interface Sci.* **166** 404
[21] Vermant J 2001 *Curr. Opin. Colloid Interface Sci.* **6** 489
[22] Lin-Gibson S, Schmidt G, Kim H, Han C C and Hobbie E K 2003 *J. Chem. Phys.* **119** 8080
[23] Hoekstra H, Vermant J, Mewis J and Fuller G G 2003 *Langmuir* **19** 9134
[24] Verduin H, de Gans B J and Dhont J K G 1996 *Langmuir* **12** 2947
[25] Vermant J, Raynaud L, Mewis J, Ernst B and Fuller G G 1999 *J. Colloid Interface Sci.* **211** 221
[26] Wang H, Lettinga M P and Dhont J K G 2002 *J. Phys.: Condens. Matter* **14** 7599
[27] Lenstra T A J and Dhont J K G 2001 *Phys. Rev.* E **63** 61401
[28] Stieger M and Richtering W 2003 *Macromolecules* **36** 8811
[29] Onuki A 1997 *J. Phys: Condens. Matter* **9** 6119
[30] Stieger M, Richtering W, Pedersen J S and Lindner P 2004 *J. Chem. Phys.* **120** 6197
[31] Senff H and Richtering W 2000 *Colloid Polym. Sci.* **278** 830
[32] Wagner N J and Russel W B 1990 *Phys. Fluids* A **2** 491
[33] Wagner N J and Ackerson B J 1992 *J. Chem. Phys.* **97** 1473
[34] Loose W and Ackerson B J 1994 *J. Chem. Phys.* **101** 7211
[35] Fuchs M and Cates M E 2002 *Phys. Rev. Lett.* **89** 248304
[36] Morfin I, Lindner P and Boue F 1999 *Macromolecules* **32** 7208
[37] Stieger M, Lindner P and Richtering W 2004 *e-Polymers* **046**